Design and Optimization of a Phase-Shifted Full Bridge DC–DC Converter with ANN Control for Photovoltaic MVDC Networks

Burugu Naveen[1], Dr.S.Narasimha [2]

[1]*PG scholar of EEE Department, TKR College of Engineering and Technology Medbowli, Meerpet, Saroornagar, Hyderabad-500097, Telangana, India,*

(burugunaveen4@gmail.com)

[2]*Associate Professor of EEE Department, TKR College of Engineering and Technology, Medbowli, Meerpet, Saroornagar, Hyderabad-500097, Telangana, India,*

(snarasimha.999@gmail.com*)*

***Abstract*—** The integration of photovoltaic (PV) sources into medium voltage (MV) DC collection networks necessitates the use of DC-DC converters with specific grid-connected capabilities. This proposed explores the implementation of a phase-shifted full bridge (PSFB) converter for MV DC collection networks in PV power plants, employing Maximum Power Point Tracking (MPPT) with Artificial Neural Networks (ANN). The unidirectional structure of the PSFB converter simplifies the design of MV circuit components. The design parameters for the PSFB converter include a power rating of 280 kW, an input voltage of 1.12 kV, and an output voltage of 19.12kV. A detailed model of the converter is developed, alongside a novel PSFB input voltage control strategy aimed at regulating the DC-link voltage.

A tuning method is proposed to account for varying transformer leakage inductance values. The performance of the PSFB converter is analysed through simulations under different PV power production profiles and MV network conditions with varying transformer leakage inductance values. The simulations confirm the efficacy of the control strategy and develop a tuning method to ensure fast stable PSFB converter operation for setting time 0.1sec and rapid power transfer stabilization across different inductance scenarios.

***Keywords*—** DC-DC power converters, MPPT with ANN Photovoltaic systems, medium voltage.

1. INTRODUCTION

The European Commission has set an ambitious target of reducing greenhouse gas emissions by 55% by 2030. Achieving this goal will require increased renewable energy adoption and enhanced energy efficiency within an integrated energy system. For instance, in France, the current 10 GW of installed photovoltaic (PV) power capacity is projected to grow to 20 GW by 2023 and 35-44 GW by 2028. This expansion necessitates the development of large-scale PV power plants, which could span many square kilometres. These large PV installations stand to benefit significantly from electrical architectures based on medium voltage direct current MVDC collection networks as shown in Figure 1.

MVDC networks offer enhanced energy efficiency compared to medium voltage alternating current MVDC collection networks. The advantages of MVDC systems extend beyond efficiency to include improved power dispatch, increased power capacity, expanded power supply range, reduced raw material consumption, lower CO2 emissions, greater network resilience, and enhanced ancillary services to the AC grid. The expected MVDC network voltage level is approximately 23 kV, though the optimal value may vary depending on power and distance requirements. Since the maximum voltage generated by PV strings typically reaches 1.8 Kv the upper limit of the low voltage range, interfacing PV strings with MVDC networks requires high-ratio DC-DC converters.

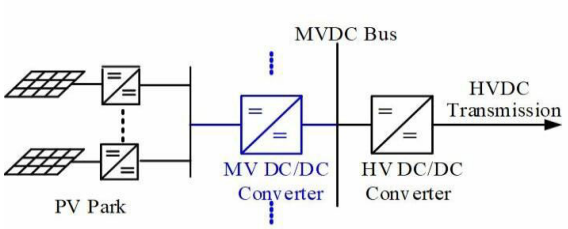

Figure 1. PV system to HVDC transmission

DC-DC converters have been extensively studied for low-voltage applications, often utilizing non-isolated buck/boost topologies. For high-power applications, suitable isolated DC-DC converter topologies include series resonant converters (SRC), LLC DC-DC resonant converters, phase-shifted full bridge (PSFB) converters, single active bridge (SAB) converters, and dual active bridge (DAB) converters, with DAB converters enabling bidirectional power flow. Isolated DC-DC converters, which use transformers operating at medium frequencies, offer significant size and weight reductions compared to equivalent power transformers operating at 50 Hz.

For medium voltage applications, DC-DC converters must meet three main requirements: power flow directionality, galvanic isolation, and modularity. Specifically, for interfacing PV strings with an MVDC network, only unidirectional power flow is required. Galvanic isolation in high-ratio DC-DC converters facilitates independent isolation coordination and grounding between LV and MV circuits and allows for optimized power electronics design. A monolithic converter is generally more cost-effective compared to a modular one, primarily due to insulation requirements.

A unidirectional, isolated DC-DC converter was previously proposed for interfacing PV strings with an MVDC network, based on the isolated boost converter topology. To enhance fault tolerance, an inductor was added at the MVDC terminals to increase output impedance to network faults such as line short-circuits. The converter featured a single maximum power point tracking (MPPT) input, whereas commercial PV inverters typically offer multiple inputs for higher granularity in energy harvesting.

We propose a unidirectional, isolated DC-DC converter that integrates multiple MPPTs each based on a boost converter and a monolithic PSFB converter for voltage step-up and galvanic isolation. The novel contribution lies in demonstrating that the simple and well-known PSFB topology is suitable for PV integration in MVDC networks. The control of the PSFB input DC-link voltage, derived from AC grid-connected converters used in PV and wind applications, is adapted for DC-DC grid-connected converters. Our control scheme, utilizing PV MPPT with ANN, regulates the LV input voltage under varying PV power and MVDC voltage conditions, unlike previous works that focused on output voltage regulation. This control scheme accounts for the leakage inductance of the PSFB converter's transformer and is beneficial for handling faults in the MVDC network, a crucial property for network-connected converters.

This propose is structured present the case study of the MVDC collection network for a PV power plant, the unidirectional isolated DC-DC converter topology, and its model, and proposes a control scheme and tuning method for input voltage regulation. Section V shows experimental results based on a reduced-scale converter prototype. One of the key contributions of this paper is the transposition of control schemes from AC-DC grid-connected converters to DC-DC grid-connected converters. The PSFB input voltage control is demonstrated to be robust and suitable for grid-connected operation, making it a promising solution for the integration of large-scale PV power plants into MVDC networks.

2. PROPOSED SYSTEM BLOCK DIAGRAM

The block diagram represents an advanced photovoltaic (PV) power collection system designed to efficiently convert solar energy into medium voltage DC (MVDC) power as shown Figure 2. The system begins with a solar PV array on the low voltage (LV) DC side, which captures sunlight and converts it into electrical energy. This LV DC power is fed into a Dual Active Bridge (DAB) converter, consisting of an inverter, transformer, and diode rectifier. The inverter, controlled by a Maximum Power Point Tracking (MPPT) algorithm implemented via an Artificial Neural Network (ANN), optimizes the power output from the PV array by adjusting to the varying solar conditions.

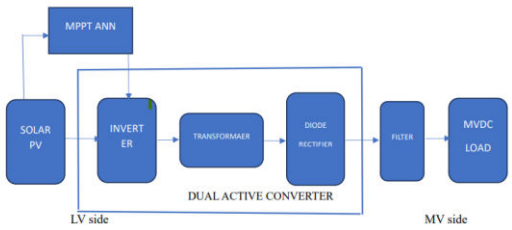

Figure 2. proposed system block diagram

The ANN processes inputs like solar irradiance and temperature to generate control pulses for the inverter switches, enabling efficient phase-shifted full bridge DC–DC conversion. The transformer in the DAB converter steps up the voltage to the MV level, providing galvanic isolation and improving power transfer efficiency. The diode rectifier converts the AC signal back to DC on the medium voltage side. Filters are employed to smooth out any switching harmonics, ensuring a stable MV DC output. This clean, high-voltage DC power is then delivered to the MV DC load, which could include industrial equipment, energy storage systems, or further distribution networks, maximizing the overall efficiency and reliability of the photovoltaic power collection system.

3.METHODOLOGY

3.1 Dual Active Bridge (DAB) Converters

Dual Active Bridge (DAB) converters are highly favoured in DC-DC power conversion due to their advantageous features, such as galvanic isolation, bidirectional power flow capability, and high efficiency achieved through soft switching. These converters are widely applied in various fields like DC microgrids, battery chargers, and solid-state transformers.

In the DAB topology, two H-bridge converters generate square waveforms applied to the primary and secondary windings of a transformer, with a controlled phase shift between them to facilitate power transfer. Initially, a single-phase shift strategy (SPS) was common, but later, the triple phase shift (TPS) strategy emerged, offering greater modulation flexibility by adjusting both duty cycles and phase shifts.

Optimizing the modulation strategy in DAB converters involves minimizing losses, particularly focusing on reducing the root mean square (rms) current through precise time-domain analysis. This approach ensures efficiency by managing conduction losses in devices and magnetic components, crucial for overall converter performance.

Designing a DAB DC-DC converter involves determining the transformer turns ratio and series inductance based on operational requirements such as regulated and unregulated port voltages, power range, and switching frequency. Strategies vary from simple methods that ensure operational controllability to advanced techniques that minimize rms current or total losses across varying operating conditions.

Recent advancements have introduced analytical approaches to optimize DAB converter designs, aiming to minimize maximum rms current under varying load conditions while ensuring soft switching. These methods employ constrained optimization techniques, leveraging algebraic equations and numerical root-finding methods to achieve optimal values for transformer parameters and inductance. Such designs not only enhance efficiency but also optimize component sizing and magnetic design, crucial for reliable converter operation across diverse applications.

The dual active bridge converter is a high-power DC-to-DC converter composed of eight MOSFET switches, a high-frequency transformer for isolation, an inductor for energy transfer, and DC-link capacitors as shown Figure 3. Its design resembles a standard full-bridge topology with a programmable rectifier, enabling bi-directional and controllable power flow. The converter includes two bridges: the primary bridge, acting as an inverter, and the secondary bridge, functioning as a rectifier. Isolation between these bridges is maintained by the high-frequency transformer, which interfaces with both sides.

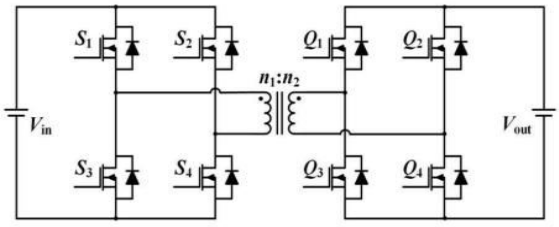

Figure 3. Dual active bridge converter

Operationally, both the primary and secondary bridges are managed simultaneously, with all switches operating at a 50% duty cycle. The

switching sequence involves diagonal pairs of switches (S1-S4 and Q1-Q4) turning on and off together, generating square waveforms at each bridge's output. Figure 3 illustrates the switching waveform, where specific pairs of switches are triggered in four interval S1, S2, Q2, and Q3 in the first interval; S1, S4, Q1, and Q4 in the second; S2, S3, Q1, and Q4 in the third; and Q2, Q3, S2, and S3 in the fourth. Typically, a phase difference of 0 to 30 degrees is maintained between the triggering of pulses from the primary to the secondary side.

This design feature allows the converter to regulate power flow bidirectionally, enhancing its utility in various high-power applications.

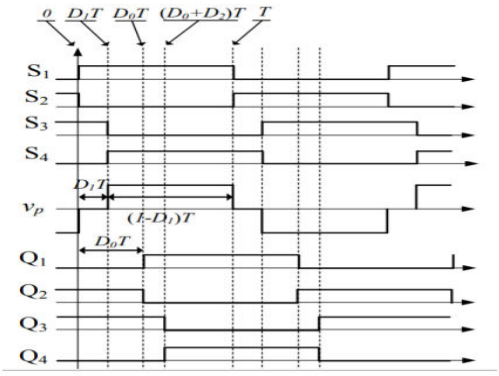

Figure 4.

The operation of the DAB converter involves complex control algorithms for achieving desired voltage and current waveforms as shown Figure 4. Here are simplified expressions

Voltage Conversion Ratio in equation 1.

$$\frac{V_{output}}{V_{input}} = \frac{N_{secondary}}{N_{primary}} \qquad (1)$$

where V_{output} is the output voltage, V_{input} is the input voltage, $N_{secondary}$ is the number of secondary windings turns, and $N_{primary}$ is the number of primary windings turns.

Power Transfer Efficiency in equation 2.

$$\eta = \frac{P_{out}}{P_{in}} \times 100\% \qquad (2)$$

where P_{out} is the output power and P_{in} is the input power.

Transformer Turns Ratio (N) in equation 3.

$$N = \frac{N_{secondary}}{N_{primary}} \qquad (3)$$

Determines the voltage conversion ratio and influences the efficiency and performance of the converter.

The Dual Active Bridge converter offers advantages of high efficiency, bidirectional power flow, and flexibility in power conversion applications. Its operation involves sophisticated control techniques to manage voltage, current, and power flow effectively.

Leakage Inductor Current Analysis in equation 4.

The leakage inductance L_{leak} in a transformer is typically expressed as a percentage of the total inductance L_{total} and can be approximated by

$$L_{leak} = L_{total} . (1 - K)^2 \qquad (4)$$

Where L_{leak} is the total inductance of the transformer, k is the coefficient of coupling between the primary and secondary windings.

3.2 PHASE SHIFTED FULL BRIDGE DC-DCCONVERTER

The full bridge converter is a type of buck-derived converter, commonly utilized in medium to high power applications due to its capability to manage substantial input voltages. It offers two primary methods for controlling output voltage: Pulse Width Modulation (PWM) control and phase shift control. The phase-shifted full bridge (PSFB) dc-dc converter is an advanced variant of the conventional full bridge dc-dc converter, distinguished by its phase-shifting control technique. This control method enables the switches in the converter to achieve zero voltage switching (ZVS), significantly reducing switching losses. As a result, the PSFB converter can achieve high efficiency at elevated switching frequencies. Additionally, this design is advantageous because

it generates low electromagnetic interference (EMI) and low switching noise, eliminating the need for additional snubber circuits to minimize losses. PSFB converters are ideal for stepping down high dc voltages and providing isolation in various medium to high power applications, including renewable energy systems, telecommunications rectifiers, battery charging systems, and server power supplies. These converters' efficient performance and reduced noise characteristics make them particularly valuable in systems where minimizing power loss and interference is critical. Furthermore, the ability to operate at high frequencies without significant efficiency losses makes PSFB converters a popular choice in modern power electronics.

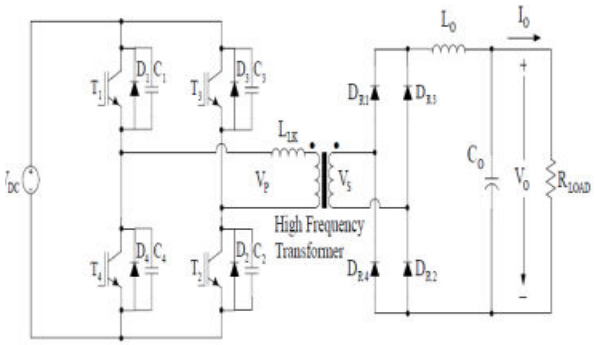

Figure 5. Phase shifted full bridge dc-dc converter

The phase-shifted full bridge (PSFB) dc-dc converter, depicted in Figure 5, is a specialized device designed to step down high voltages, making it ideal for medium to high power applications. This converter consists of a full bridge inverter, a high-frequency transformer, a full bridge diode rectifier, and a low-pass filter at the output. The gating signals are applied to the switches in a phase-shifted manner to enable zero voltage switching (ZVS) operation, which reduces switching losses and enhances efficiency. The full bridge inverter is composed of four semiconductor switches, typically insulated-gate bipolar transistors (IGBTs) or metal-oxide-semiconductor field-effect transistors (MOSFETs), each paired with diodes. In the phase-shifted control scheme, the gate signals for switches T2 and T3 are phase-shifted relative to those for T1 and T4, ensuring efficient ZVS operation.

A high-frequency transformer is utilized to transfer energy, and the high-frequency AC voltage at the secondary side is rectified using a full-wave rectifier. The resulting DC output voltage is then smoothed by a low-pass filter. Parasitic capacitances (C1, C2, C3, C4) are present across the switches, contributing to the overall circuit behavior. Additionally, an inductor is connected in series with the primary winding of the transformer to emphasize the leakage inductance of the high-frequency transformer. If necessary, an extra inductor can be added in series with the transformer's primary winding to further enhance this effect.

The interaction between the switch output capacitance and the transformer's leakage inductance, while generally detrimental in hard switching converters, is advantageous in the PSFB converter. This interaction helps to achieve ZVS, thereby eliminating switching losses and improving the overall performance of the converter. This makes the PSFB topology particularly suitable for medium to high power applications, such as renewable energy systems, data centres, and industrial power supplies, where efficiency and reliability are critical. Additionally, the PSFB converter's ability to minimize electromagnetic interference and maintain stable operation under varying load conditions enhances its applicability in sensitive electronic environments.

3.3 Photovoltaic (PV) Module

Solar PV (photovoltaic) modules are devices that convert sunlight directly into electricity through the photovoltaic effect. These modules typically consist of interconnected solar cells made from semiconductor materials, such as silicon. When sunlight strikes the solar cells, it excites electrons, generating an electric current as shown in Figure 6.

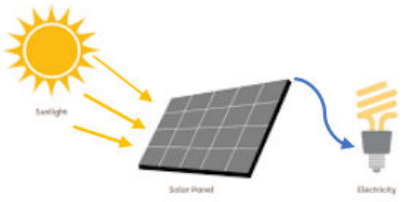

Figure 6. Solar PV (photovoltaic) modules

Mathematically, the power output P_{PV} of a solar PV module is determined by its open-circuit voltage V_{OC} and short-circuit current I_{SC} in equation 5.

$$P_{PV} = V_{OC} \times I_{SC} \quad (5)$$

Here, V_{OC} is the voltage across the module when no current is flowing (open circuit), and I_{SC} is the maximum current the module can deliver (short circuit).

The efficiency ηPV of a solar PV module indicates how effectively it converts sunlight into electricity in equation 6.

$$\eta PV = \frac{P_{PV}}{P_{IN}} \times 100\% \quad (6)$$

Where P_{IN} is the incident power from sunlight. Efficiency varies based on factors such as cell quality, temperature, and sunlight intensity.

The energy output E_{PV} of a solar PV module over a period t is given in equation 7.

$$E_{PV} = P_{PV}.t \quad (7)$$

This formula calculates the total energy produced by the module over time t.

Solar PV modules are widely used in various applications, including residential rooftops, commercial installations, and large-scale solar farms. They offer a renewable and sustainable energy solution with minimal environmental impact, contributing significantly to global efforts towards clean energy adoption.

4. ANN BASE CONTROL STRATEGY

The propose an optimized controller using an artificial neural network (ANN) technique to develop a high-performance controller. A typical feed-forward ANN structure is depicted in Figure 7. This structure consists of several neurons, which are analogous to biological brain cells. These neurons are organized in layers and have numerous weighted connections with neurons in successive layers.

Each input layer neuron receives a set of data from the input variables and sends them to the hidden layer neurons. The hidden layer neurons combine these inputs to form a single result, which is then delivered to the output layer through an activation function. Finally, each output layer neuron adds the hidden layer's outputs to the bias and passes the result via the activation function to generate the final output.

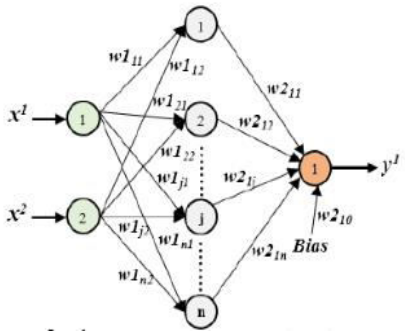

Figure 7. Artificial neural network (ANN) technique

As shown in Figure 7, x represents the input of the ANN, y is the output, and w denotes the weights and biases. The final output is formulated by using linear activation functions for the neurons of the input and output layers, and sigmoidal activation functions for the neurons of the hidden layer in equation 8.

$$\boldsymbol{Y_1} = \boldsymbol{W2_{10} + W2_{11}z_1} + \boldsymbol{W2_{12}z_2} + \ldots\ldots + \boldsymbol{W2_{1n}z_{n2}} \quad (\mathbf{8})$$

therefore, the generalized output equation can be expressed as follows in equation 9.

$$Y_1 = \sum_{j=0}^{n} w_{221j} z_j \quad (9)$$

Where

$$z_0 = 1$$

$$z_j = f(a_j) = \frac{1}{1 + e_{aj}}$$

$$a_j = \sum_{h=w1jh}^{2} x^h$$

During neural network training, the weights of layers are modified to achieve the values

the goal of finding a set of weights that minimizes the error between the ANN's output and the target value.

The mean square error (MSE) is the ANN network's performance function, which is determined in in equation 10.

$$E_{mse} = \frac{1}{N}\sum_{i=1}^{N}(t_i - y_{i1})^2 \qquad (10)$$

where t_i represents the target at sample i, y_i represents the output signal at sample i, and N is the training number of models.

5.SIMULATIN

I developed a comprehensive simulation model in Simulink focusing on the phase-shifted full bridge (PSFB) converter controlled by a Maximum Power Point Tracking (MPPT) algorithm integrated with an Artificial Neural Network (ANN) as shown Figure 8.

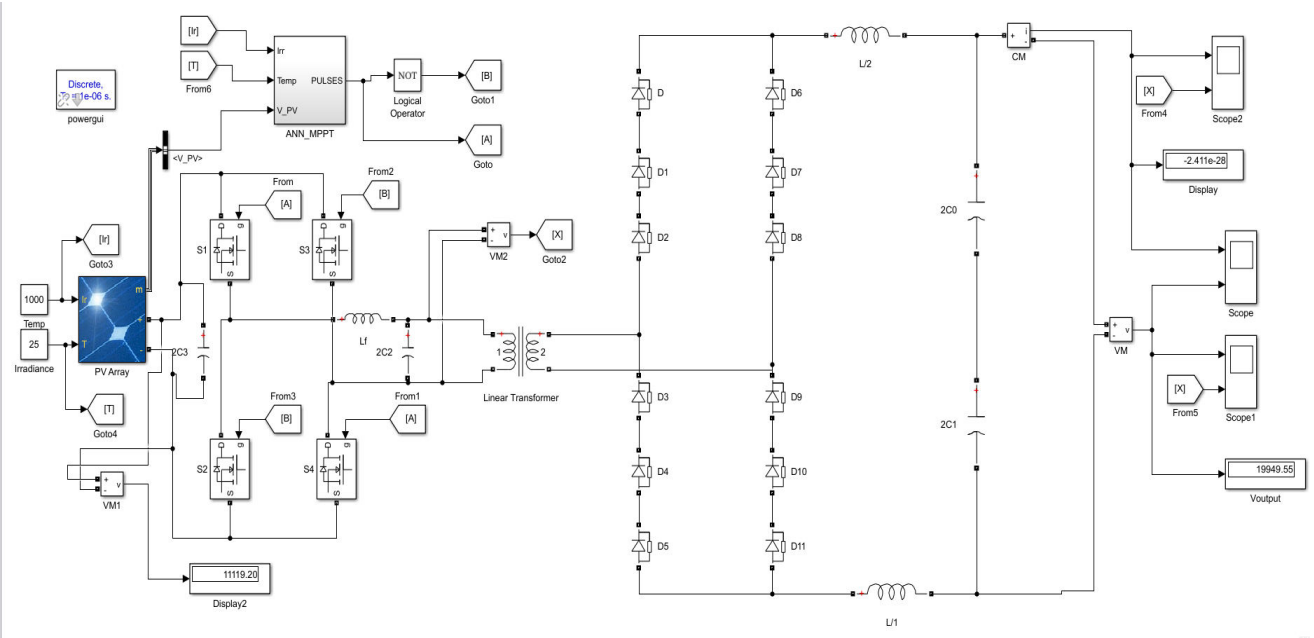

Figure 8 Model created to proposed system

This model is designed for application within photovoltaic (PV) solar systems, specifically addressing the integration of PV sources into medium voltage (MV) DC collection networks. The PSFB converter plays a crucial role in efficiently managing the power conversion process, ensuring optimal performance and reliability. The MPPT-ANN control mechanism dynamically adjusts the operating point of the PV system to maximize power output, adapting to varying environmental conditions. This innovative approach enhances the efficiency and stability of grid-connected PV systems, contributing significantly to the advancement of sustainable energy technologies.

Network (ANN) within the phase-shifted full bridge (PSFB) converter represents a sophisticated method to enhance the efficiency of photovoltaic (PV) systems. The MPPT algorithm, crucial for maximizing the power output from PV panels, is dynamically optimized by the ANN, which is trained to predict the optimal operating point under varying environmental conditions. This intelligent control mechanism ensures that the PV system consistently operates at its maximum power point, even as irradiance and temperature fluctuate.

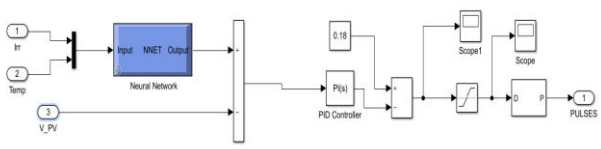

Figure 9. ANN Created in simulation

The ANN-enhanced MPPT algorithm generates precise control pulses for the inverter in the PSFB converter, which adjusts the phase shifts to

regulate the power conversion process. This results in improved efficiency, reduced switching losses, and enhanced overall performance of the PV system as shown in Figure 9. The combination of MPPT and ANN in this context ensures robust, adaptive, and efficient energy conversion, making it a significant advancement in solar energy technology.

6.SIMULATIN RESULTS

Medium Voltage (MV) DC collection networks for photovoltaic (PV) power plants, a Phase-Shifted Full Bridge (PSFB) converter is employed due to its high effectiveness and ability to manage large power levels. The performance of this converter can be optimized using Maximum Power Point Tracking (MPPT) implemented through Artificial Neural Networks (ANN). This approach allows the system to dynamically adjust to changing environmental conditions, ensuring that the maximum power is always extracted from the PV panels.

In the designed photovoltaic (PV) solar system, the configuration comprises 400 parallel strings, each consisting of 300 series-connected modules. The system operates under an irradiance value of 1000 W/m² and an ambient temperature of 25°C. Under these specified conditions, the PV array generates an output voltage of 1.120 kV, as illustrated in the waveform analysis as shown in Figure 10. This substantial voltage output is achieved through the optimal arrangement and connection of the PV modules, which maximizes energy collection and effectiveness of energy conversion.

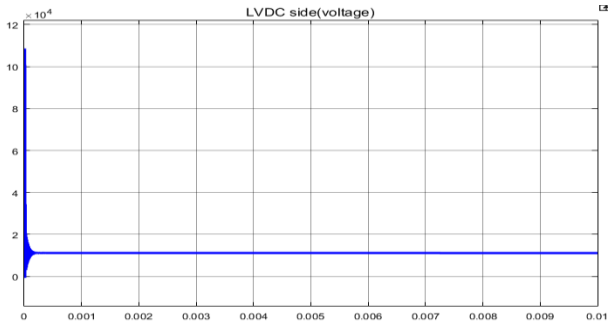

Figure 10. PV Output voltage (LVDC)

The typical ANN structure for MPPT includes an input layer that receives data from solar PV, one or more hidden layers that perform complex computations and feature extraction, and an output layer that provides the optimal duty cycle or reference voltage for the DC-DC converter. The ANN training process involves collecting a comprehensive dataset under different environmental conditions from the solar PV, preprocessing the data for normalization, and then training the ANN using algorithms such as backpropagation and gradient descent. The trained ANN is subsequently validated and tested with separate datasets to ensure it generalizes well to new, unseen data. One of the primary advantages of using ANNs for MPPT is their high accuracy in predicting the maximum power point (MPP) under rapidly changing environmental conditions.

The precise Artificial Neural Networks (ANN) control pulses generated for the inverter in the phase-shifted full bridge (PSFB) converter optimize the power conversion process, contributing to the highly effectiveness and voltage fast stability of the overall PV system for MV collection network. This output voltage serves as a crucial parameter for integrating the PV system into medium voltage MVDC collection networks, demonstrating the system's capability to meet the demanding requirements of modern renewable energy applications.

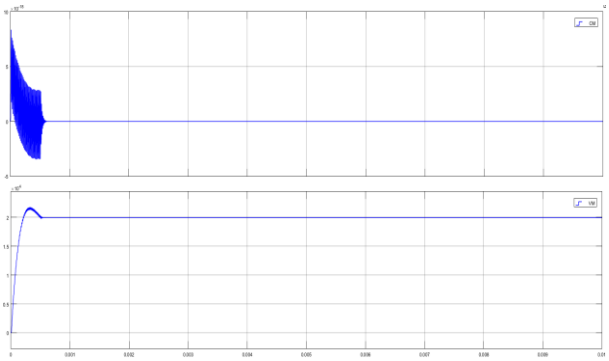

Figure 11. Output medium voltage MVDC & current

As a result, the output voltage from the PSFB converter is significantly boosted to 19.12 kV the converter is developed, alongside a novel PSFB input voltage control strategy aimed at regulating the DC-link voltage from 1.120kv to 19.12kv for MV networks, which is suitable for medium voltage DC (MVDC) applications. This output is depicted in the waveform Figure 11, highlighting the system's capability to effectiveness convert and step up the voltage for

grid integration and other high-voltage applications. The advanced control and conversion techniques employed in this system demonstrate its potential for enhancing the effectiveness and reliability of renewable energy solutions on environmental changes.

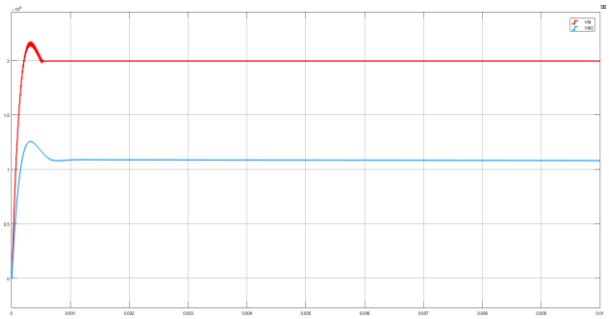

Figure 12. Output voltage and Voltage before PSFB converter

The output voltage from the PSFB converter is significantly boosted to 19.12 kV, suitable for medium voltage DC (MVDC) applications. Comparative waveform analysis is performed, with one waveform illustrating the inverter output controlled by the MPPT-ANN in the PSFB converter and the other depicting the output at the MVDC side Figure 12.

The simulations results confirm the effectiveness of the control strategy, develop a tuning method to account for varying transformer leakage inductance values 1mH the stable operation condition Output voltage as shown in Figure 13

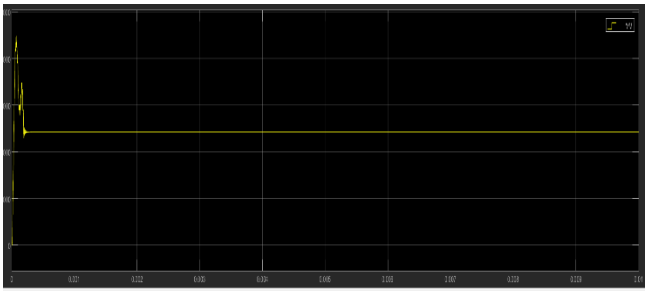

Figure 13 Output voltage using leakage inductance 1mH.

The Output voltage by using leakage inductance 20mH the stability of the output voltage is greater compared to 1mh as shown in Figure 13.

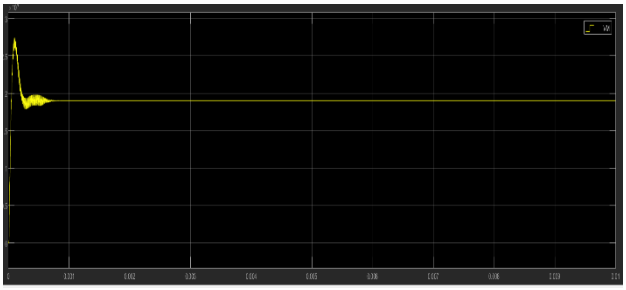

Figure 13 Output voltage using leakage inductance 20mH.

The Output voltage by using leakage inductance 50mH the stability of the output voltage is better compared to 1mh and 20mh as shown in Figure 14. For ensuring the PSFB converter maintains stable operation at output voltage and rapid power transfer across different inductance scenarios.

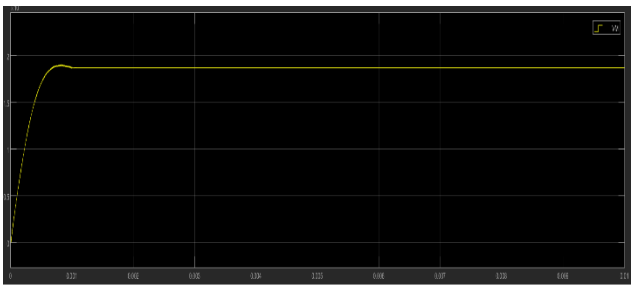

Figure 14. Output voltage using leakage inductance 50mH.

A critical aspect of the PSFB converter's performance is its response to different inductance values. In this study, the output voltage oscillations were analysed for three different inductance values: 1H, 20H, and 50H. The key performance metrics considered were rise time, settling time, and peak overshoot. variable inductance values lead to reduced oscillations and peak overshoot, improving the overall stability of the converter

For an inductance of 1H, the system exhibited a rise time of 0.01 seconds and a settling time of 0.1 seconds, with significant oscillations and a high peak overshoot. Specifically, the output voltage showed two oscillations with substantial peak overshoot, indicating a response but potential stability issues. When the inductance was increased to 20H, the rise time increased to 0.02 seconds, while the settling time remained at 0.1 seconds. The output voltage showed only one oscillation with a moderate peak overshoot, suggesting a more balanced response and improved stability compared to the 1H inductance. For the highest inductance value of 50H, the rise time further increased to 0.03 seconds, with the settling time still at 0.1 seconds. The output voltage exhibited one oscillation with a low peak

overshoot, implying the highest stability observe on Table.1.

S. NO.	Inductance (H)	Rise Time (s)	Peak Overshoot	Oscillation Magnitude	Settling Time (s)	Observations
1	1H	0.01	High	High	0.1	Significant oscillations
2	20H	0.02	Moderate	Moderate	0.1	Reduced oscillations
3	50H	0.03	Low	Low	0.1	Minimal oscillations

Table.1.

By increasing leakage inductance values (e.g., to 20 H or 50 H) to dampen oscillations, using high-quality components that can withstand high-frequency oscillations, implementing advanced control algorithms like ANN to handle oscillations effectively and conducting regular maintenance checks to identify and replace stressed components before they fail. By addressing high oscillations and implementing these measures, the performance and reliability of MV DC voltage collection networks in PV power plants can be significantly improved.

7.CONCLUSION

The integration of phase-shifted full bridge (PSFB) converters controlled by Maximum Power Point Tracking (MPPT) algorithms with Artificial Neural Networks (ANNs) represents a significant advancement in PV solar system technology under different environmental conditions, especially for medium voltage (MV) DC collection networks. This approach facilitates effectiveness power conversion from PV output to medium voltage (MV) DC collection networks and optimal energy harvesting from PV arrays under varying environmental conditions by Artificial Neural Networks (ANNs). The simulation results demonstrate that the PSFB converter, with its tailored control strategy, effectively regulates DC-link voltages from 1.120kv to 19.12kv and the simulations results confirm the efficacy of the control strategy, develop a tuning method to account for varying transformer leakage inductance values(1Mh,20Mh,50mH), The Output voltage by using leakage inductance 50mH the fast stability of the output voltage is better compared to 1mh and 20mh at setting time 0.1sec. By enhancing voltage conversion effectiveness and reliability, this innovative system contributes to the advancement and viability of sustainable energy solutions in PV power plants.

The PSFB converter effectively steps up the PV array's output voltage to 19.12 kV, suitable for MVDC applications, demonstrating enhanced effectiveness and reliability in converting and integrating renewable energy into grid-connected systems. This approach represents a significant advancement in sustainable energy technologies, offering promising solutions for future PV power plant implementations.

REFERENCES

[1] European Commission. The European Commission'S Priorities. Accessed: Jul. 26, 202. [Online]. Available: https://ec.europa.eu/info/ strategy/priorities-2019-2024_en

[2] S. Narasimha, T.Srinika "ANN based fast charging architecture with V2G and G2V" The International journal of analytical and experimental modal analysis Vol. XV, Issue No. VIII, pp. 436-443, ISSN No:0886-9367, August2023.

[3] D. Salel and F. Delpit, ''Etat du photovoltaïque en France,'' Ademe, Angers, France, 2019.

[4] Dr.s. Narasimha, Dr.S. Surrender reddy 3" Dynamic and hybrid phase shift controller for dual active bridge converter" International Journal of Engineering & Technology, Volume 7, Issue 4, Feb. 2019. ISSN 2227-524X. pp:4795-4800.

[5] A. Cabrera-Tobar, E. Bullich-Massagué, M. Aragüés-Penalba, and ¯ O. Gomis-Bellmunt, ''Topologies for large scale photovoltaic power plants,'' Renew. Sustain. Energy Rev., vol. 59, pp. 309–319, Jun. 2016.

[6] H. A. B. Siddique, S. M. Ali, and R. W. De Doncker, ''DC collector grid configurations for large photovoltaic parks,'' in Proc. 15th Eur. Conf. Power Electron. Appl. (EPE), Sep. 2013, pp. 1–10.

[7] S. Narasimha, D.Spandana " A Closed Loop Hybrid Phase Shift Controlled Dual Active Bridge Converter with Dynamic Input Voltage Change" International Journal of Electrical Electronics & Computer Science Engineering, Volume 4, Issue 5, 2017),E-ISSN : 2348-2273, P-ISSN : 2454-1222,pp23-26.

[7] P. Le Metayer, J. Paez, S. Toure, C. Buttay, D. Dujic, E. Lamard, and P. Dworakowski, ''Break-even distance for MVDC electricity networks according to power loss criteria,'' in Proc. 23rd Eur. Conf. Power Electron. Appl. (EPE ECCE Europe), Sep. 2021, pp. 1–9.

[8] K. Tytelmaier, O. Husev, O. Veligorskyi, and R. Yershov, ‘‘A review of non-isolated bidirectional DC–DC converters for energy storage systems,’’ in Proc. Int. Young Scientists Forum Appl. Phys. Eng. (YSF), Oct. 2016, pp. 22–28.

[9] F. C. Schwarz and J. B. Klaassens, ‘‘A controllable 45-kW current source for DC machines,’’ IEEE Trans. Ind. Appl., vol. IA-15, no. 4, pp. 437–444, Jul. 1979.

[10] J. Zhang, W. Jiang, T. Jiang, S. Shao, Y. Sun, B. Hu, and J. Zhang, ‘‘A three-port LLC resonant DC/DC converter,’’ IEEE J. Emerg. Sel. Topics Power El1etron., vol. 7, no. 4, pp. 2513–2524, Dec. 2019.

[11] L. H. Mweene, C. A. Wright, and M. F. Schlecht, ‘‘A 1 kW 500 kHz frontend converter for a distributed power supply system,’’ IEEE Trans. Power Electron., vol. 6, no. 3, pp. 398–407, Jul. 1991.

[12] S. Narasimha, D. Ushasri, “AN EFFICIENT CONTROLLER FOR GRID CONNECTED PV SYSTEM WITH IMPROVED POWER QUALITY” A Journal Of Composition Theory(Jct),Volume:15, Issue:10, Page No:253-266, Issn:0731-6755, Year:2022.

[13] K. Park and Z. Chen, ‘‘Analysis and design of a parallel-connected single active bridge DC–DC converter for high-power wind farm applications,’’ in Proc. 15th Eur. Conf. Power Electron. Appl. (EPE), Sep. 2013, pp. 1–10.

[14] J. Xue, F. Wang, D. Boroyevich, and Z. Shen, ‘‘Single-phase vs. threephase high density power transformers,’’ in Proc. IEEE Energy Convers. Congr. Expo., Sep. 2010, pp. 4368–4375.

[15] R. W. A. A. De Doncker, D. M. Divan, and M. H. Kheraluwala, ‘‘A three-phase soft-switched high-power-density DC/DC converter for high-power applications,’’ IEEE Trans. Ind. Appl., vol. 27, no. 1, pp. 63–73, Jan. 1991.

[16] M. Mogorovic and D. Dujic, ‘‘100 kW, 10 kHz medium-frequency transformer design optimization and experimental verification,’’ IEEE Trans. Power Electron., vol. 34, no. 2, pp. 1696–1708, Feb. 2019.

[17] I. Villar, L. Mir, I. Etxeberria-Otadui, J. Colmenero, X. Agirre, and T. Nieva, ‘‘Optimal design and experimental validation of a mediumfrequency 400 kVA power transformer for railway traction applications,’’ in Proc. IEEE Energy Convers. Congr. Expo. (ECCE), Sep. 2012, pp. 684–690.

[18] G. Ortiz, J. Biela, D. Bortis, and J. W. Kolar, ‘‘1 megawatt, 20 kHz, isolated, bidirectional 12 kV to 1.2 kV DC–DC converter for renewable energy applications,’’ in Proc. Int. Power Electron. Conf., Jun. 2010, pp. 3212–3219.

[19] P. Dworakowski, P. Le Metayer, C. Buttay, and D. Dujic, ‘‘Unidirectional step-up isolated DC–DC converter for MVDC electrical networks,’’ Presented at CIGRE Session, 2022.

[20] J. D. Paez, J. Maneiro, S. Bacha, D. Frey, and P. Dworakowski, ‘‘Influence of the operating frequency on DC–DC converters for HVDC grids,’’ in Proc. 21st Eur. Conf. Power Electron. Appl. (EPE ECCE Europe), Sep. 2019, p. 10.

[21] H. Wang, Y. Zhou, X. Huang, Y. Wang, and H. Xu, ‘‘Topology and control strategy of PV MVDC grid-connected converter with LVRT capability,’’ Appl. Sci., vol. 11, no. 6, p. 2739, Mar. 2021.

[22] E.-S. Park, S. J. Choi, J. M. Lee, and B. H. Cho, ‘‘A soft-switching active-clamp scheme for isolated full-bridge boost converter,’’ in Proc. 19th Annu. IEEE Appl. Power Electron. Conf. Expo., Feb. 2004, pp. 1067–1070.

[23] SG250HX Multi-MPPT String Inverter for 1500 Vdc System, Sungrow, Datasheet, 2019. [Online]. Available: https://www.bath.ac. uk/publications/library-guides-to-citing-referencing/attachments/ieeestyle-guide.pdf

[24] J. M. S. Callegari, A. F. Cupertino, V. D. N. Ferreira, and H. A. Pereira, ‘‘Minimum DC-link voltage control for efficiency and reliability improvement in PV inverters,’’ IEEE Trans. Power Electron., vol. 36, no. 5, pp. 5512–5520, May 2021.

[25] L. Huang, C. Wu, D. Zhou, and F. Blaabjerg, ‘‘Comparison of DC-link voltage control schemes on grid-side and machine-side for type-4 wind generation system under weak grid,’’ in Proc. 47th Annu. Conf. IEEE Ind. Electron. Soc., Oct. 2021, pp. 1–6.

[26] S. F. Zarei, H. Mokhtari, M. A. Ghasemi, S. Peyghami, P. Davari, and F. Blaabjerg, ‘‘DC-link loop bandwidth selection strategy for gridconnected inverters considering power quality requirements,’’ Int. J. Electr. Power Energy Syst., vol. 119, Jul. 2020, Art. no. 105879